Neutron Scattering of Annealed Solution-Grown Crystals of Polyethylene†

David M. Sadler

H. H. Wills Physics Laboratory, University of Bristol, Tyndall Avenue, Bristol BS8 1TL, England

Stephen J. Spells*

Department of Applied Physics, Sheffield City Polytechnic, Pond Street, Sheffield S1 1WB, England. *Received November 15, 1988; Revised Manuscript Received March 21, 1989*

ABSTRACT: Neutron scattering from annealed solution-grown crystals of polyethylene at $q \sim 0.1$–0.8 Å^{-1} is used to study the chain conformation, in particular the changes that can be inferred during the annealing process. Particular emphasis is placed on the case of lamellar thickening by a factor of about 2, which is known to occur without migration of centers of gravity of molecules. It is found that the conformation within the folded sheets changes by the least amount possible, consistent with the increase in stem lengths and the consequent decrease in their number. The annealed conformation can be obtained from the unannealed one by removing stems randomly throughout each molecule, leaving the lateral dimensions of the folded sheets unchanged. From these results it can be inferred that there is no melting in any proper sense during this type of annealing. These results are fully consistent with previous measurements of molecular dimensions. For the particular case of deuterated matrix material, where no measurements of molecular dimensions are possible, the changes in intensity do not agree quantitatively with those expected from the changes in lamellar spacings. It is concluded that, in these cases, heterogeneity, which is well documented for annealed crystals, is such that there are crystal regions containing more than average hydrogenous "label", which thicken less than the average for the whole samples. Infrared spectroscopic results for the same samples are presented in the following paper, providing further information on these conformational changes.

Introduction

The formation of crystals of polymers can take place either as the result of primary crystallization from the liquid and solution states (usually as chain-folded lamellae) or by modifying existing crystals. Annealing, or heat treatment, generally modifies the structure by lamellar thickening and an increase in crystallinity. We report conformational studies here on crystal thickening in the solid state of crystals grown originally from solution.[1,2] The results are probably relevant to other annealing processes, e.g., isothermal thickening[3,4] (lamellar thickening at the crystallization temperature shortly after the initial creation of the crystals).

Neutron scattering (NS) has been used to obtain detailed models for the chain conformation of solution-crystallized polyethylene (PE) crystals.[5-12] One of the most recent and detailed models[12] is the basis for the present work. We argue that the scattering data and infrared spectroscopy *combined with* independent information (e.g., the existence of stems, the straight chain traverses of the lamellae) leave very little ambiguity in determining the arrangement in space of stems from the same molecule. This arrangement defines in large degree the nature of the folding (see below). This approach also holds for the present work, which involves an extension to annealed solution grown crystals.

We have applied two "labeling" techniques, NS and mixed-crystal infrared spectroscopy (IR),[13] on the same samples and with a closely integrated interpretation. This paper describes the NS results and interprets the conformation after annealing in terms of the one before.

The As-Crystallized Conformations. The sheetlike form of the scattering units was recognized at an early stage of applying NS, followed by the phenomenon of superfolding of the chain-folded ribbons back on themselves, leading to multiple sheet arrangements, and of dilution of the growth face with other molecule(s). Evidence from intermediate-angle NS, e.g., ref 5, 6, and IR[14,15] indicated a dilution of 50%. Dilution by an integer factor (2 in this case) can be interpreted as the folded sheet being formed from that number of molecules (e.g., 2). The most recent NS work[12] shows that the scattering data for a wide range of molecular weights can be interpreted by using the same statistical distribution of molecular stems along the growth face. This distribution involves a probability p, which gives the preference for adjacent reentry ($p = 0.75$). The stem sequences can be defined in terms of whether a current site is occupied by the molecule in question. The probability of finding the same molecule at the next (adjacent) site is p, and for an occupancy of the folded sheet of 0.5 the probability of finding the other "partner" molecule at that site is $1 - p$. The only parameter to be changed on variation of molecular weight is the number of sheets occupied. The average molecular weight per sheet was found to be about 20 000 by fitting calculated curves to the experimental data. A schematic representation of the chain conformation is given in Figure 1. An important feature of the as-crystallized structure is the existence of groups of stems (see also the stacked-sheet model of Stamm and collaborators[7-9]). The group in general extends over several sheets, including typically 5–20 stems. For the special case of one sheet the probabilities of various group sizes are given by simple formulas: there is a simple distribution of group lengths along each sheet. The probability of having n stems in a row is p^{n-1}; that of having n and no more is $p^{n-1}(1 - p)$. The average group length L_g within one infinite sheet is defined by $a/(1 - p) = 4a$, where a is the interstem distance. For finite length sheets the average of L_g is less than this value. There is a fairly high probability of groups in adjacent sheets being partially

† The work described in this paper represents a combined study undertaken over several years. David Sadler pursued the analysis of the neutron scattering results in 1987 and early 1988 and prepared an initial manuscript on which the present neutron scattering paper is largely based. I subsequently continued to analyze the infrared data and to make comparisons with molecular model calculations. Sadly, David's tragic death in 1988 prevented him from seeing how these fit his own conclusions. Consequently, the comparison of results from the two techniques and the conclusions drawn are the work of Stephen Spells.

0024-9297/89/2222-3941$01.50/0

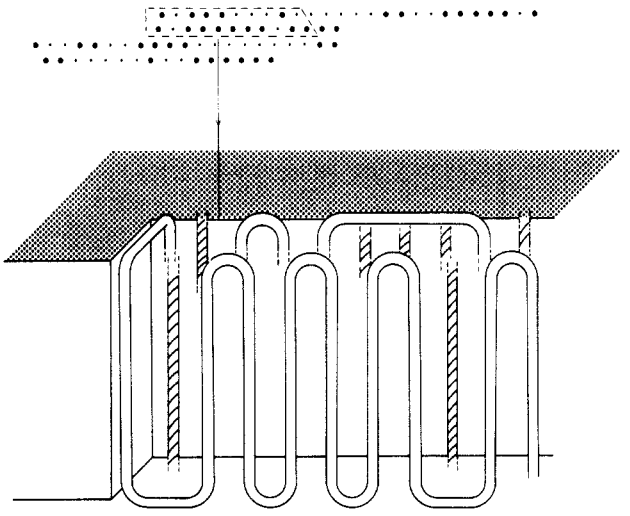

Figure 1. Schematic three-dimensional sketch of the conformation in solution-grown crystals prior to annealing.[14] At the top is shown the structure as projected on to the {001} plane, with the larger dots representing stems from one molecule.

in register, which means that the average group contains more than four stems. The group sizes for single sheets will be related to these values even in the more general case of groups extending over several sheets.

Annealing Processes. On the basis of a number of observations, a working hypothesis is that there are at least three regimes of annealing: reversible and irreversible changes that do not affect the lamellar periodicity l, an intermediate regime that may involve a solid-state thickening process, and partial melting at the highest annealing temperature (T_a). The evidence for the existence of a thickening process with no melting has tended to be rather indirect; recently it has been suggested that for fast rates of heating to T_a at least, there is generally a significant loss of crystallinity during annealing.[17,18] On the other hand, NS has shown that for T_a = 123 °C the centers of gravity of molecules are not mobile during annealing, whereas for T_a = 125 °C they are.[19] This conclusion is made on the basis of an isotope segregation effect that occurs as a result of annealing at the higher T_a values but not at the lower ones. In these experiments and the present ones the rates of heating to T_a were not high (10 deg min^{-1}). The criterion of mobility of entire molecules is taken as the operational definition of the regime of thickening: below a demarcation value T_{al} of T_a, there is no such mobility. The existence of mobility may or may not correlate with the loss of crystallinity during annealing. The changes in l for $T_a < T_{al}$ may typically be from 110 Å for crystals grown from xylene at 70 °C to 300 Å for $T_a \simeq 124$ °C. In many cases the changes in l represent about a factor of 2 and this may not be a coincidence (see also below).

The criterion of molecular mobility leads to the idea of a length L_a, which defines the length scale over which the sample is simultaneously molten at any given T_a. It is reasonable to presume that for $T_a > T_{al}$, molten regions of dimensions L_a exist during annealing that are larger than the molecular size (e.g., as characterized by the radius of gyration R_g), whereas for $T < T_{al}$, then $L_a < R_g$ (e.g., for a solid-state annealing process with no truly molten regions).

Experimental evidence from sedimented crystal monolayers is not directly applicable to the sedimented mats used here, since electron microscope studies have shown different behavior where crystals overlap.[20] On annealing suspensions of crystals in silicone oil, holes developed above a critical temperature of 118 °C.[21] Again, the effect of lamellar contact is shown by the growth of holes being more rapid where two crystals were in contact, although the critical temperature for hole formation was the same.

Many studies have documented the increase in average small-angle X-ray (SAX) repeat distance l both with T_a and time of annealing (e.g., the original work where l was found to increase logarithmically with time[2]). Evidence has accumulated that there is also a marked heterogeneity on annealing, consistent with the larger width of the SAX maxima, which often involves a doubling of l. Rather than l increasing over the whole sample from its initial value l_0, some regions thicken faster than others: analysis of wide-angle (002) diffraction peaks[22,23] showed the presence of crystal thicknesses of l_0, $2l_0$, and $3l_0$. Evidence for $l = 2l_0$ also came from SAX measurements.[24] Similar conclusions have come from measurements using the longitudinal acoustic mode technique: either there is a very broad distribution of stem lengths[25] or even a double population.[26] For the case of nylon 66, the simultaneous existence of l_0 and $2l_0$ can be seen by SAX,[27] and on the basis of the tendency for $l = 2l_0$, a pulling through of folds model was proposed by Dreyfuss and Keller.[28]

Small-angle NS measurements were made on solution-grown PE crystals[19] after annealing. Values for the radius of gyration were determined both in and out of the plane of lamellae (R_x and R_z, respectively). R_x remained approximately constant during annealing. R_z increased with increasing T_a. This is to be expected on the basis of lamellar thickening, and, for both unannealed crystals and those for which T_a = 123 °C, the R_z and l values are consistent with each molecule being confined to individual lamellae. (For $T_a < 123$ °C there was further evidence of heterogeneity in the samples, the ratio of R_z to l being higher than for both unannealed samples and those with T_a = 123 °C.)

Peterlin[29] has given a rather general approach to annealing on the basis of an activation energy for stem lengthening that is proportional to the stem length. This implies that each region of the crystals thickens fairly abruptly. This is consistent with the evidence of heterogeneity, in that the sample will generally consist of a mixture of unannealed and annealed structures (plus perhaps partly annealed structures). There is on the other hand no evidence in support of the entire assembly of lamellae thickening continuously and in concert.

Experimental Details

Sample Preparation and Characterization. The preparation of mixed-crystal mats of PE from xylene solution has been described previously.[5b] In all cases, a crystallization temperature of 70 °C was used. To optimize the ratio of signal to background, a deuterated PE (PED) matrix was used (DM) for intermediate- and wide-angle measurements. A hydrogenated PE (PEH) matrix (HM) was used for small-angle work. Dried oriented mats were pressed below the crystallization temperature to minimize void scattering. Samples cut to the necessary dimensions were annealed on a Mettler hot stage, with a heating rate of 10 °C/min.

The molecular weight of PE starting materials, prepared by liquid–liquid fractionation, were determined by GPC. Long spacings were measured by Raman spectroscopy (LAM) and small-angle X-ray diffraction. The lamellar orientation was monitored at the small-angle X-ray facility at the Synchrotron Radiation Source (Daresbury). Results are shown in Figure 2. Broad peaks were seen by using the LAM method, but no bimodal distribution of stem lengths was apparent.[25]

Neutron Scattering Experiments. We divide the scattering experiments into three angular ranges:[12] (i) small angle (SANS) $q < 0.1$ Å^{-1}, the D17 multidetector instrument (ILL) was used here; (ii) intermediate angle (IANS) $0.4 > q > 0.1$ Å^{-1}; D17 was used; (iii) wide angle (WANS) $q > 0.4$ Å^{-1}. The single-detector guide tube diffractometer (Harwell) was used in this region.[32]

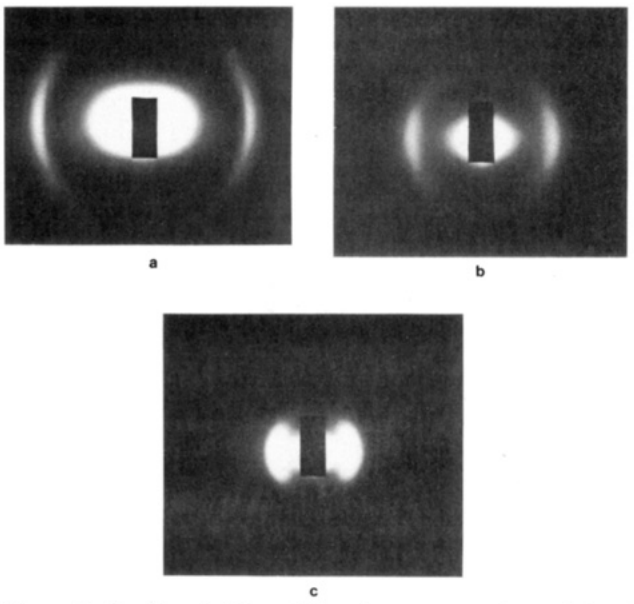

Figure 2. Small-angle X-ray diffraction patterns of annealed and unannealed crystals: (a) unannealed, (b) annealed at 115 °C for 60 min, (c) annealed at 122 °C for 60 min.

Some measurements were also taken on D1B at ILL.

Samples of dimensions 10 × 10 mm or 20 × 7 mm were cut out and stacked in apertures in cadmium holders. For SANS and IANS measurements, thin quartz plates on either side of the cadmium holder held the sample in position. For WANS measurements, thin aluminum foil served this purpose. Data were obtained for samples, blank runs with PEH and PED of similar weight to the isotopes in samples, and an empty cell.

Neutron Scattering Analysis.[30] If the average scattering length for hydrogen isotopes is $\bar{b}$, then the scattering length for isotope i may be written as $\bar{b} + \delta b_i$. With n hydrogen atoms per molecule and the scattering function $P_k(q)$ for a single molecule, it can be shown that

$$|A(q)|^2 = |A_0(q,\bar{b})|^2 + \sum_k \delta b_k{}^2 (n^2(P_k(q)))N_k \qquad (1)$$

where N_k is the number of molecules of isotope k and $A_0(q,\bar{b})$ corresponds to the coherent scattering amplitude for the average isotopic concentration.

Before using eq 1, instrumental corrections (see below) and subtraction of the incoherent background must be carried out. For PEH matrix samples (HM, 3% PED), $|A_0(q,\bar{b})|^2$ makes a small contribution and can reasonably be approximated to the signal from a PEH blank of the same weight. For PED matrix (DM) measurements where the equality $\bar{b} \simeq b_H$ is no longer valid, it becomes necessary to use the actual value of $\bar{b}$.

Rewriting eq 1 in terms of the macroscopic scattering cross section, $d\Sigma/d\Omega$, we obtain

$$V\frac{d\Sigma}{d\Omega} = |A_0(q,\bar{b})|^2 + N(nP(q))c_D c_H(b_D - b_H)^2 \qquad (2)$$

where V is the sample volume and c_H and c_D are the volume fractions and b_H and b_D, the scattering lengths for PEH and PED. The normalized intensity $I(q)$ is then $nP(q)$.

As in earlier work,[2] the incoherent scattering from pure PEH and from water was used to calibrate the intensity.

Calculation of the Scattered Intensity from a Correlation Function $\Gamma(R)$. As in the work on solution-grown crystals before annealing,[5,12] the organization of most monomer units within crystal stems can be utilized effectively for simplifying calculations. It was shown in that work[12] that the scattered intensity can be expressed in terms of the correlation function $\Gamma(R)$ for crystal stems with a separation of R as

$$I_c(q) = \frac{n_L\pi}{q}\int \Gamma(R)J_0(qR)\,dR \qquad (3)$$

where n_L is the number of labeled atoms per unit length of crystal stem. This equation involves an integral over all crystal stems, without taking into account the atomic structure within the stems. This form is convenient for computation, provided the experimental intensities being compared are accordingly modified. The modification involves calculating the scattering from one stem (using the Debye relationship for isotropic samples) and the scattering from long thin stems with no systematic correlation between them:

$$I_c(q) = n_L\pi/q \qquad (4)$$

If the ratio of intensity from a real stem to that from a thin stem is denoted by $C(q)$, then the experimental intensities, $I(q)$, can be modified to give equivalent intensities, $I_c(q)$, for infinitely thin stems being $I_c(q) = I(q)/C(q)$. With this modification, experimental intensity data can be directly compared with calculations made from eq 3 for model systems. Scattering measurements are again plotted in the form of $I_c(q)q^2$ versus q^2 in this work. As noted previously,[12] the calculations based on eq 3 are only valid for $q > 1/l$ where l is the stem length. This approach gave accurate agreement for isotopic mixtures of paraffins where the scattering should be given by eq 4, for randomly arranged stems.

The integral in eq 3 includes $R = 0$, i.e., the "self"-correlation of each stem with itself as in eq 4. Equation 3 can be rewritten to make explicit the distinction between intra- and interstem correlations:

$$I_c(q) = \frac{\pi}{q}(1 + \Gamma'(q)) \qquad (5)$$

where

$$\Gamma'(q) = \int \Gamma'(R)J_0(qR)\,dR$$

where $\Gamma'(R)$ now excludes $\Gamma(0)$ and represents the systematic interference between stems as a consequence of folding. As discussed previously,[12] on a plot of $I_c(q)q^2$ versus q the positive and negative contributions to $\Gamma'(q)$ approximately cancel over a sufficiently large q range. Stems which cluster together lead to increased values of $I_c(q)q^2$ at small q and a corresponding decrease at large q. Hence in fitting data to predictions, we give priority to the shape of the plot rather than to absolute intensities.

Generating Correlation Functions $\Gamma(R)$. Stem positions $\mathbf{R}_i$ were generated by a Monte Carlo procedure[12] according to whichever model is considered (see below). A fraction of the stem pairs was sampled and a histogram calculated for the probability of any given stem separation $|\mathbf{R}_i - \mathbf{R}_j|$ (equivalent to $\Gamma(R)$). Several "molecules" were generated and the histogram is averaged over them.

The Effects of Crystal Orientation and Amorphous Material. The method of sedimenting and filtering single-crystal suspensions produces a preferential and reproducible orientation of lamellar normals in the direction of the mat normals. The quantification of this effect and its influence on the enhancement of scattering by comparison with isotropic samples was discussed previously.[12] It was concluded that the enhancement factor for sufficiently large q was of the order of 1.8.

The single-crystal mats show crystallinities of about 0.75, from DSC measurements. The fraction of material in the form of disordered loops on the crystal surfaces is likely to produce minimal scattering over most of the wavevector range used.[12] This correction for the amorphous material is probably a slight overestimate, since some of the lack of complete order is accounted for by relatively tight folds (see above). As a first approximation, the experimental scattering intensities may therefore be divided by the crystallinity fraction and also by the enhancement factor by crystal orientation. From the values quoted, the combined correction is close to unity for single crystals.

Small-angle X-ray patterns (Figure 2) show that the long spacing changes appreciably for annealing temperatures up to 122 °C for the PED matrix. However, the degree of orientation of lamellae, as indicated by the azimuthal spread of the small-angle peak, is only slightly reduced over this range of T_a. Patterns such as these are analyzed in more detail elsewhere.[18] On this evidence, values for the correction factor need not be changed from values for unannealed single crystals. Longitudinal acoustic mode results

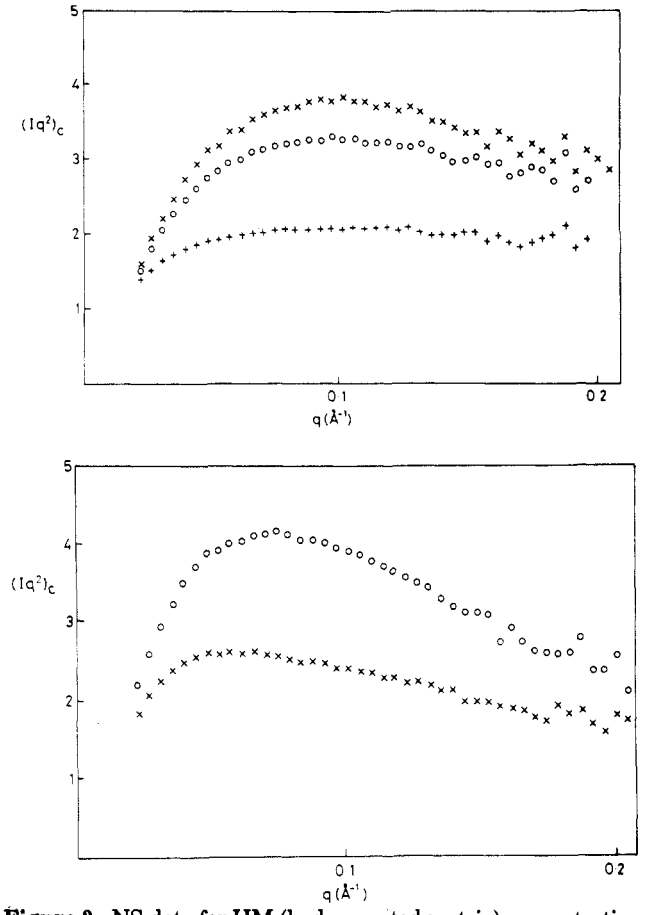

Figure 3. NS data for HM (hydrogenated matrix) concentration c_D of deuterated label 0.03. (a, Top) Molecular weight 93 000; (×) unannealed, (○) annealed T_a = 112 °C, (+) annealed T_a = 123 °C. (b, Bottom) Molecular weight 380 000; (○) unannealed; (×) annealed T_a = 123 °C.

show a wide distribution of stem lengths, but not a bimodal distribution.

Results

NS scattering data in the small-angle region, for HM, are shown in Figure 3. This covers the range where the scattering vector $q \simeq 1/(\text{stem length})$ so that the calculations for "long" stems become invalid. Nevertheless, the effect of annealing in reducing scattering intensities throughout the region is evident, the intensity decreasing with increased annealing temperature (T_a), approximately in proportion to the ratio l_0/l.

Data for the intermediate-angle region for DM samples are shown in Figure 4a. The intensities are similar for samples with c_H = 0.03 and 0.1 but the intensity is significantly reduced for c_H = 0.2. This behavior is also reflected in data for samples annealed at 120 °C for 1 h (Figure 4b). The low intensity from c_H = 0.2 compared with c_H = 0.1 is probably the result of isotopic fractionation, an effect that is enhanced by increasing the concentration of the minority species. This is because fractionation leads to c_D and c_H being no longer constant over the sample so that the sample consists of a number of microsamples, each with its own local concentration. Equation 2 gives the maximum intensity, in this q range, for uniform c_D and c_H. In order to quantify this effect, it is necessary to specify the way that c_H is not constant over the sample—the simplest assumption being for part of the sample to contain no hydrogenous "label" (c_H = 0). On this basis, comparing c_H values of 0.03 and 0.2 and assuming homogeneity for c_H = 0.03, eq 2 would imply that the actual value of c_H in the remaining labeled part of the

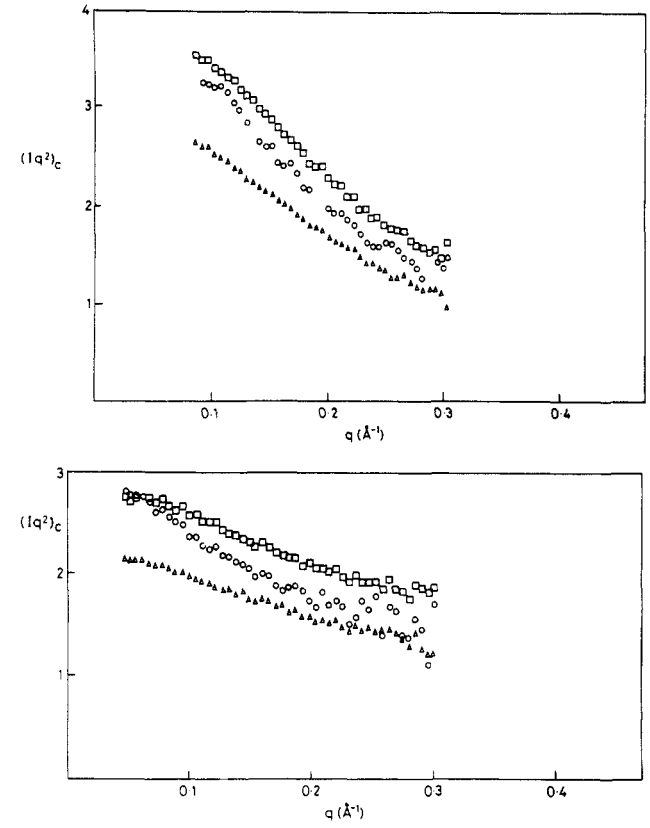

Figure 4. NS data for deuterated matrix (DM), $\bar{M}_w$ of hydrogenous label = 103 000: (a, top) unannealed for (□) c_H = 0.03, (○) c_H = 0.1, (△) c_H = 0.2; (b, bottom) annealed at T_a = 120 °C for 1 h, (○) c_H = 0.03, (□) c_H = 0.1, (△) c_H = 0.2.

sample would be 0.4 for the case of an average over all the sample of c_H = 0.2. This estimate is a lower limit to the likely enhancement effect on c_H, since it assumes homogeneity for c_H = 0.03. The effect of c_H on the intensity could also be partly due to a mismatch in molecular weights of the isotopic species.[32] The distortion of the data from these sources is probably not significant if c_H = 0.4 is excluded, but the effect of heterogeneity on annealing is (see the section on this subject below). For unannealed crystals the intensities agree well in the region of overlap of q for HM and DM (c_D = 0.03 (Figure 4a)). However, for annealed crystals the intensities are significantly higher for c_H = 0.03 (Figure 4b compared with Figure 3).

Figure 5 shows data for $q < 0.8$ Å^{-1} for annealed and unannealed crystals for two molecular weight values. Although there are changes in intensities (e.g., reductions at smaller q), the changes are less than for HM data. The fact that difference data can be obtained for such large q reflects the fact that the inherent contrast is very high for CH_2/CD_2 and that the coherent (diffuse) background is reasonably low. The fact that self-consistent data can be obtained to q = 0.8 Å^{-1} shows that the systematic errors for background subtraction for $q \lesssim 0.4$ Å^{-1} are small, since the signal after background subtraction is smaller by a factor of more than 4 for q = 0.8 Å^{-1} compared with 0.4 Å^{-1}.

Interpretation in Terms of Conformations. As Crystallized. Figure 6 shows results of calculations for a series of p values. In contrast to previous calculations,[12] we include no correlation between the folding statistics in adjacent rows. For high p values there is a convexity of the $(Iq^2)_c$ curves at smaller q, and for low p values there is a marked minimum followed by a marked increase in intensity at large q. The limiting case of a peak at the next-but-one neighbor separation ($q = 2\pi/8.8$ Å^{-1}) is only

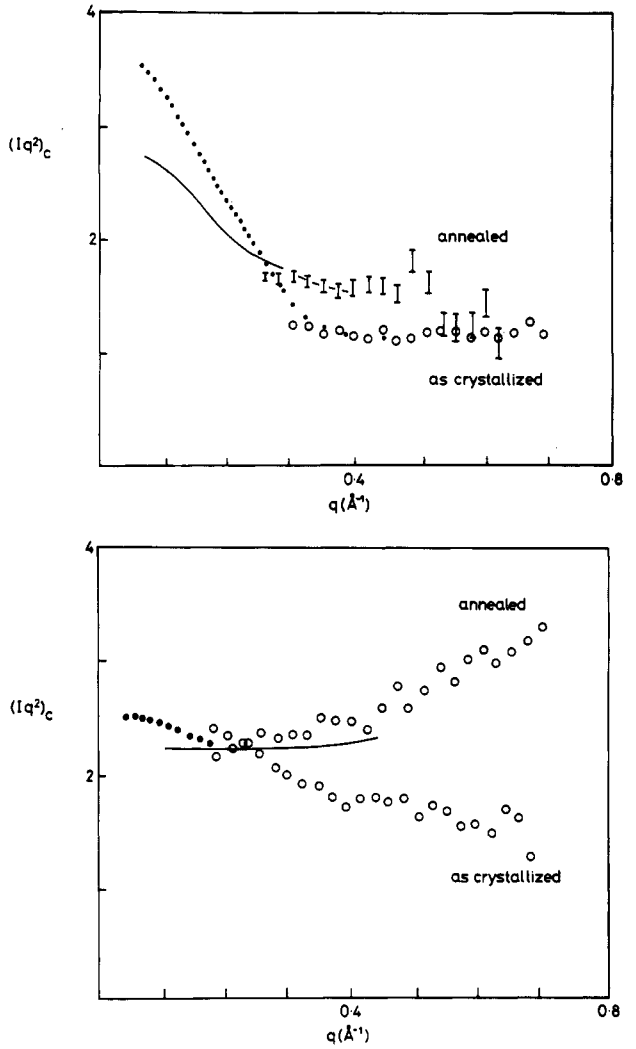

Figure 5. NS data for DM, for the largest q values, using more than one detector configuration. (a, Top) • and O, unannealed; solid line and I, annealed at T_a = 120 °C for 1 h; $\bar{M}_w$ of hydrogenous label = 103000. (b, Bottom) Solid circles and lower open circles, unannealed; solid line and upper open circles, annealed at T_a = 120 °C for 1 h; $\bar{M}_w$ of hydrogenous label = 87000.

achieved at $p \lesssim 0.05$ (cf. ref 12). These trends are readily interpreted: for $p > 0.5$ a preferred length enters the problems related to the group size L_g. Here we refer to the group as the set of adjacent stems within one sheet, or the "single-sheet group" as we have called it in the following paper.[13] For example, $p = 0.75$ can be related to a distribution for L_g with a characteristic distance corresponding to four stems (17.6 Å). An enhancement of intensity around $q \simeq 2\pi/17.6$ Å^{-1} (or somewhat higher for a finite sheet) is therefore to be expected. For small p values the stems of the same molecule avoid each other while still occupying half the sheets—hence the preference for next-but-one neighbor correlations.

The general balance of intensity at the larger and smaller q values in Figure 6 and the absence of a dramatic minimum and maximum at q of 0.4 and 0.8 Å^{-1}, respectively, favor $p \simeq 0.75$, significantly greater than 0.5 (the value for random occupation within the sheets). IR results also strongly favor $p \simeq 0.75$. Low values of $\simeq 0.25$ can be excluded since the size of groups would then be extremely small, leading to very little splitting of the relevant IR bands (see also ref 13). $p \simeq 0.75$ does not, however, give an optimum fit for $q < 0.4$ Å^{-1} (see also Yoon and Flory[6]), but this would not seem sufficient evidence to disregard the other evidence for $p \simeq 0.75$.

The conformation is illustrated schematically in Figure 1 (three dimensions) and in Figure 7a (two-dimensional representation of one sheet).

Changes on Annealing. Annealing increases the average length of the stems: hence the number of stems decreases and the intramolecular correlations between stems are bound to decrease unless the molecule shrinks laterally. The consequence is clearly seen in Figures 4 and 5, since they can be interpreted in terms of a decrease in the interference terms $\Gamma'(R)$ and $\Gamma'(q)$ (see also below). Two questions summarize the more detailed information:

(1) Does the q dependence of $\Gamma'(q)$ change on annealing? (2) What are the magnitudes of changes in $\Gamma'(q)$? The second question depends primarily on the degree of annealing of the crystal regions containing the minority ("label") isotopic species: a quantitative analysis of both DM and HM results requires the recognition, already well established, that annealed crystal samples are often markedly heterogeneous in terms of annealing (see below).

The q dependence of $\Gamma'(q)$ gives information on any changes in interstem correlations there may be on annealing. Removal of stems randomly within each molecule, starting from the original conformation, is the simplest way of reducing the number of stems (Figure 7b). The effect on the scattering is very simple: to reduce $\Gamma'(R)$ and $\Gamma'(q)$ in proportion to $\Gamma(0)$ and its Fourier transform $\Gamma'(0) = 1$ (Figure 6b, solid lines). This procedure represents a relatively large "memory" of the original stem arrangements in the as-crystallized materials. Depending on the way in which labeled stems are connected, such a process may be difficult to envisage, due to topological constraints (e.g., with one fold on the top surface of the crystal, another on the bottom, etc.). Nevertheless, its simplicity provides a good starting point for calculations. A second type of structure will be given as an example of a more fundamental change in stem arrangements: that produced by removing stems from the ends of groups (Figure 7c). (c) differs from (b) primarily concerning the fate of larger groups, e.g., at each end of the structure in (a). The scattering can be calculated according to the following considerations (applied to groups of stems along individual rows of stems). In the as-crystallized folded sheet, the probability of finding a group of size $2n$ is proportional to p^{2n-1}. This will also be the probability of finding a group of size n in the annealed structure, which originates from the groups of $2n$. Hence the scattering can be calculated by using a modified value of p that is just equal to p_0^2, where p_0 is for the unannealed crystals. The overall occupancy of the stems in the rows is reduced from 0.5 in the original crystals to 0.25 (for $l/l_0 = 2$). Results (broken line) are included in Figure 6b, with a change in the q dependence of $\Gamma'(q)$. Such a change does not seem consistent with either HM or DM results. It can be seen that the scattering is no longer that characteristic of sheets, even at smaller q. This is because the low occupancy (0.25) and the relatively high p value (0.57) lead to large gaps between groups, so that the overall sheetlike conformation is lost in this model. Clearly, the data favor random dilution and the retention of the overall sheet shape, rather than the more substantial stem rearrangements.

The degree of annealing can be considered to be determined by the increase in stem length and a proportionate decrease in the number of stems. The total occupancy of the rows of the original folded sheets reduces from 0.5 to a lower value. The length of stems can be measured from small-angle X-ray periodicities l and from R_z values.[19] For HM samples the ratios of l/R_z remain constant for T_a = 123 °C, but this equivalence of stem length measure-

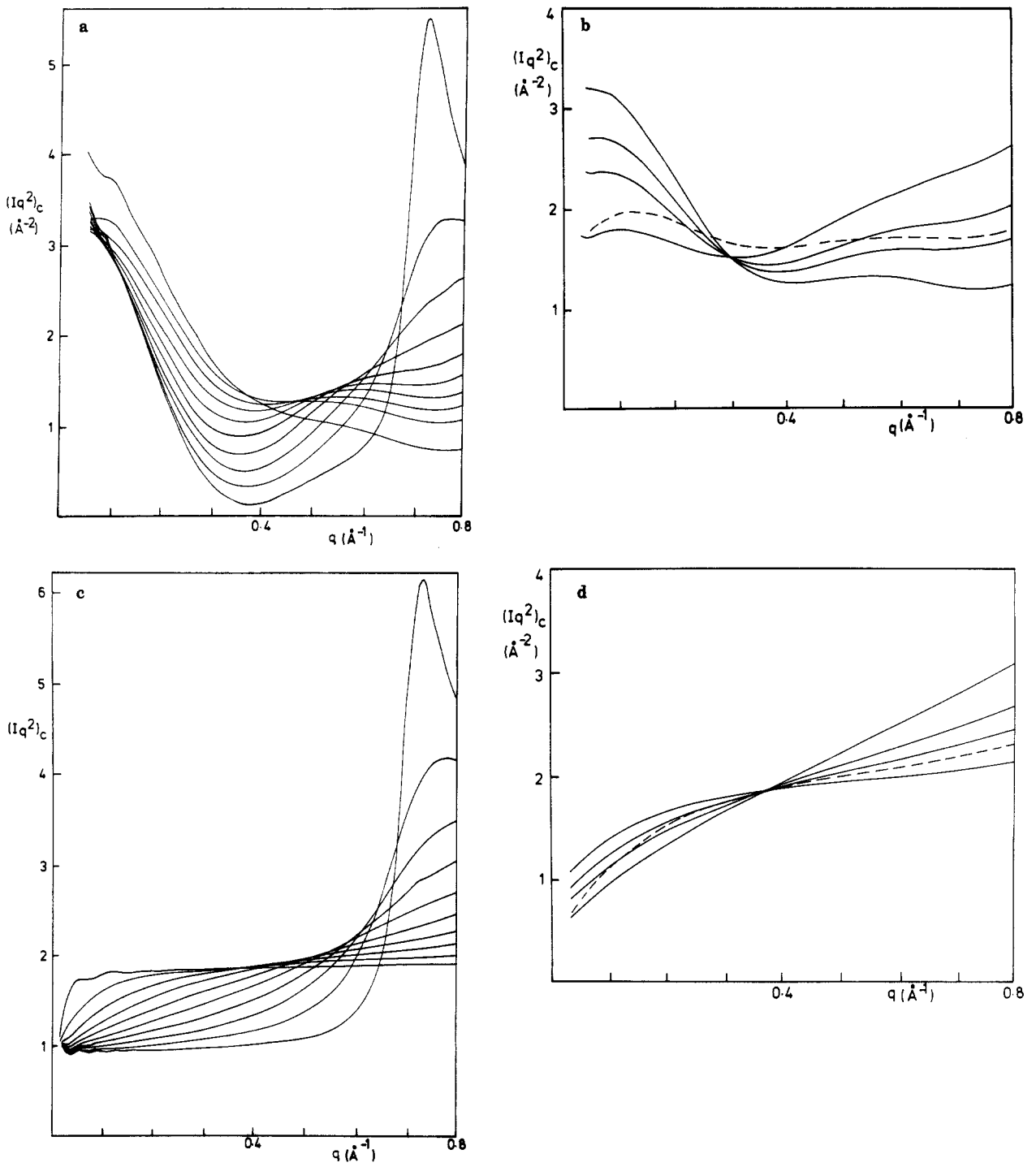

Figure 6. Calculated NS data, using the methods described in the analysis section, directly comparable with the data in Figures 3–5. (a) Solid lines, occupancy of sheets 0.5, p values in steps of 0.1 from 0.05 to 0.95, 20 stems in each of four sheets. (b) Broken line, occupancy 0.25, $p = (0.75)^2$; solid lines derived from an occupancy of 0.5, $p = 0.75$, by diluting intensity contribution $\Gamma'(q)$ from the interstem correlations by a factor of 1.2, 1.5, and 2, corresponding to 20 stems in each of four sheets. (c) As (a), but with 20 stems in one sheet. (d) As (b), but with 20 stems in one sheet.

ments may not hold for DM where R_z values are not obtainable. For HM and $T_a = 123$ °C, $l_0/l = 0.5$, so that since the lateral dimensions R_x remain constant,[19] the overall stem occupancy should decrease from 0.5 to 0.25. For the case of removal of stems, which is random within each molecule, the resultant $\Gamma'(q)$ can be obtained simply by scaling down $\Gamma'(q)$ by 2. For the q range in Figure 4, $\Gamma'(q)$ represents most of the intensity so that a reduction of $\Gamma'(q)$ by 2 leads to a decrease in $\Gamma(q)$ by 2, which can be seen to be consistent with these data.

For DM, however, even when $l_0/l \simeq 0.5$, the changes in $\Gamma'(q)$ are much less (by factors of about 1.2–1.4). The only way to resolve this apparent anomaly is to recall that annealing leads to considerable heterogeneity and that concentrations c_H up to 0.4 may well change annealing properties, as explained below.

The morphological changes on annealing have been noted earlier. For sedimented mats involving stacked lamellae, the annealing process is expected to involve some degree of cooperative motion in neighboring lamellae, despite the heterogeneity noted above. No decrease in density is observed after annealing single-crystal mats, so it must be concluded that vacancies produced in thickened crystals are filled in this way.

Consequences of the Isotope Effect. It has long been established that use of the isotope labeling technique re-

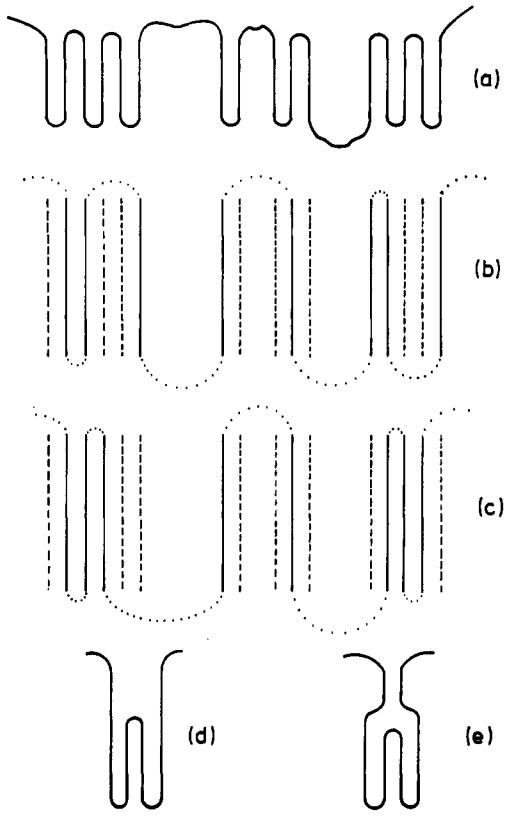

Figure 7. Schematic representations of the conformations within each sheet: (a) unannealed (as in Figure 1); (b) annealed using random removal of stems, predictions in b or d of Figure 6, solid lines; (c) annealed by using the shrinkage of groups from their extremities (cf. predictions, broken line in b or d of Figure 6.

quires account to be taken of the nonzero thermodynamic differences, due to the factor of 2 difference in mass between hydrogen and deuterium. Deuteration causes a 4-deg decrease in the melting point of PE. It is fair to summarize the position by contrasting effects involved in changing molecular position and molecular conformation. An isotopic mixture is a polymer blend: it is well-known that the entropy *of mixing* is extremely small ($\sim k$ per molecule), so that minute energetic differences according to isotope can lead to nonrandom mixing in equilibrium[33] and, in limiting cases, phase separation into two phases of different isotope concentration. Segregation according to kinetic differences[5,14,30] in crystalline systems is also likely to be significant since growth rate is an exponential function of supercooling. By contrast, there is no evidence of significant conformational changes according to isotope: indeed this is unlikely a priori. For example, the *configurational* entropy in the liquid is $\sim Nk$ per molecule where N is the number of effective links, so that energetic effects that could change conformation would have to be correspondingly large.

Hence, although we may well have a lack of random mixing within a sample, the molecular conformations of both isotopic species are almost certainly representative of pure isotopic species. The effects of lack of random mixing are 2-fold. (1) If the length scale of isotope concentration fluctuation corresponds to the range of resolution of the NS instrument, an (usually additional) intensity contribution will occur, which increases steeply with decreasing q. (The random-phase approximation[34] applies to the fluctuation length being less than the molecular size.) (2) If the regions of different isotope concentrations c_H and c_D are large enough, the sample can be considered as a composite of "microsamples" (see above); the total intensity will thus be reduced since the maximum of $\langle c_H c_D \rangle$ corresponds to homogeneity. In practice, this may well be a rather unimportant effect for the scattering data, especially since there are other uncertainities related to the absolute calibration of intensities. However, variations in the concentrations are likely to be very significant for annealing properties as explained in the following, because of the combined effects of heterogeneity and isotope effect.

In some cases (see Introduction) the average l value is thought to be made up of contributions from l_0, $2l_0$, and $3l_0$ and in any event a wide distribution of stem lengths. It is also clear that the label isotopic concentration can vary over a sample.[5,14] For DM this implies that the (hydrogenous) label is preferentially in those parts of the sample that anneal least readily. The very presence of local label concentrations of ~ 0.4 (see above) may well itself increase differences in "annealability". There is no very obvious reason why the effects of heterogeneity are larger for DM than for HM. However, one possibility is based on the fact that the roles of the two isotopes are not symmetric: in DM the H material will presumably tend to crystallize first whereas for HM the D material will probably tend to be more concentrated at the lamellar perimeters.[5b] It is reasonable that on the average the annealing will tend to start from the edge of crystals rather than the centers. Whatever the detailed effects involved, full self-consistency is obtained in the case of HM, where results for R_x and R_z and heterogeneity of isotope[19] are obtainable on the same samples as for the intensity data at relatively large q (Figure 4). For DM only large q results are obtained, so no comparison is possible with R_x and R_z data on the same samples. Futhermore the IR results[13] show the same effects: for DM the "label" molecules appear to be much more similar to the unannealed case compared with HM, for equivalent values of l_0/l.

It is worth noting that the randomness of stem removal discussed so far only relates to randomness *within each molecule*. If in DM samples, for example, half the H molecules anneal with stem lengths doubling, whereas the other half remain unaffected, this could still give "random" removal, with $\Gamma'(q)$ reducing by a factor of 0.25. By contrast, the well-documented evidence of sample heterogeneity means that stems are not likely to be removed randomly *over the whole sample*.

Changes in Stem Positions during Annealing. The molecules retain the overall sheet shape as defined for the unannealed crystals, with the same length of sheet as measured by R_x, but with an increase in R_z in proportion to the increase in stem lengths. The pattern of stem removal within the sheets is such as to keep the q dependence of $\Gamma'(q)$ the same as before, which indicates that within the molecule the removal of stems is random. This suggests that the lateral translation of stems during annealing is limited—less than, for example, would be necessary if each group of stems in the original conformation were to shrink so as to keep itself as compact as possible. For $l = 2l_0$, groups of size $4n$ (n an integer) could readily be changed to those of $2n$ by using a "pulling through of folds" mechanism,[28] so as to give virtually no net translations of stems. However, other groups would require a net loss or gain of stem material to adjoining groups along the molecule (see Figure 7). Presumably these necessary translations to adjust group sizes are not such as to tend to increase or decrease adjacency on average. One can also infer that as folds pull through the crystal (Figure 7d), the stems on either side probably do not have a tendency to shrink in toward each other as shown in Figure 7c. If this were the case, large groups would tend to shrink laterally, giving a higher degree of adjacency than for the (observed)

random dilution. The general conclusions that lateral displacements of stems are minimized tend to support the view that for the type of annealing studied here the rearrangement is a solid-state one, involving no melting even on a local scale. In the following paper it is shown that the infrared data, at least for higher guest molecular weights, favor the shrinkage of groups from their ends, and the models are discussed further.[13]

Acknowledgment. We are very grateful to Professor Andrew Keller for his sustained interest and encouragement throughout this work and to the staff of the Institut Laue Langevin (Grenoble) and AERE (Harwell, in particular Vic Rainey) for assistance with neutron scattering measurements. We also thank the staff of the SRS (Daresbury) for assistance with X-ray diffraction measurements and SERC for financial support for S.J.S.

References and Notes

(1) Keller, A.; O'Connor *Discuss. Faraday Soc.* **1958**, *25*, 114.
(2) Fischer, E. W.; Schmidt, G. F. *Angew. Chem.* **1962**, *74*, 551.
(3) Weeks, J. J. *J. Res. Natl. Bur. Stand.* **1963**, *67A*, 441.
(4) Martinez-Salazar, J.; Barham, P. J.; Keller, A. *J. Mater Sci.* **1985**, *20*, 1616.
(5) (a) Sadler, D. M.; Keller, A. *Polymer* **1976**, *17*, 37-40. (b) Sadler, D. M.; Keller, A. *Macromolecules* **1977**, *10*, 1128-1140. (c) Sadler, D. M.; Keller, A. *Science* **1979**, *203*, 263.
(6) Yoon, Y.; Flory, P. *Discuss. Faraday Soc.* **1979**, *68*, 288.
(7) Stamm, M.; Fischer, E. W.; Dettenmaier, M.; Convert, P. *Discuss. Faraday Soc.* **1979**, *68*, 263.
(8) Dettenmaier, M.; Fischer, E. W.; Stamm, M. *Colloid Polym. Sci.* **1980**, *258*, 343.
(9) (a) Wignall, G. P.; Mandelkern, L.; Edwards, C.; Glotin, M. *J. Polym. Sci., Polym. Phys. Ed.* **1982**, *20*, 245. (b) Stamm, M. *J. Polym. Sci., Polym. Phys. Ed.* **1982**, *20*, 235.
(10) Summerfield, G. C.; King, J. C.; Ullman, R. *J. Appl. Crystallogr.* **1978**, *11*, 534.
(11) Sadler, D. M. *J. Appl. Crystallogr.* **1983**, *16*, 579.
(12) Spells, S. J.; Sadler, D. M. *Polymer* **1984**, *25*, 739-748.
(13) Spells, S. J.; Sadler, D. M. *Macromolecules*, following paper in this issue.
(14) Spells, S. J.; Sadler, D. M.; Keller, A. *Polymer* **1980**, *21*, 1121.
(15) Spells, S. J.; Keller, A.; Sadler, D. M. *Polymer* **1984**, *25*, 749-758.
(16) Spells, S. J. *Polym. Commun.* **1984**, *25*, 112-165.
(17) Grubb, D. T.; Liu, J. J. H.; Coffrey, M.; Bilderbeck, D. M. *J. Polym. Sci., Polym. Phys. Ed.* **1984**, *22*, 367.
(18) Spells, S. J.; Hill, M. J., unpublished results.
(19) Sadler, D. M. *Polym. Commun.* **1985**, *26*, 204.
(20) Holland, V. F. *J. Appl. Phys.* **1964**, *35*, 3235.
(21) Roe, R. J.; Gieniewski, C.; Vadimsky, R. G. *J. Polym. Sci., Polym. Phys. Ed.* **1973**, *11*, 1653-1670.
(22) Windle, A. H. *J. Mater. Sci.* **1975**, *10*, 252.
(23) Windle, A. H. *J. Mater. Sci.* **1975**, *10*, 1959.
(24) Waters, A. D. V.; Windle, A. H. *J. Mater. Sci.* **1976**, *11*, 1577.
(25) Synder, R. G.; Scherer, J. R.; Reneker, D. H.; Colson, J. P. *Polymer* **1982**, *23*, 1286.
(26) Alamo, R.; Mandelkern, L. *J. Polym. Sci. B, Polym. Phys. Ed.* **1986**, *24*, 2087.
(27) Burmester, A. F.; Dreyfuss, P.; Geil, P.; Keller, A. *J. Polym. Sci., Polym. Lett. Ed.* **1972**, *10*, 769.
(28) Dreyfuss, P.; Keller, A. *J. Polym. Sci., Polym. Lett. Ed.* **1970**, *8*, 253.
(29) Peterlin, A. *J. Polym. Sci., Polym. Lett. Ed.* **1963**, *1*, 279.
(30) Sadler, D. M. In *Crystalline Polymers*; Hall, I., Ed.; Applied Science: London, 1984.
(31) Haywood, B. C. G.; Worcester, D. L. *J. Phys. E* **1973**, *6*, 568.
(32) Akcasu, A. Z.; Summerfield, G. C.; Jahshan, S. N.; Han, C. C.; Kim, C. Y.; Yu, H. (1980) *J. Polym. Sci., Polym. Phys. Ed.* **1980**, *18*, 863.
(33) Bates, F. S.; Wignall, G. D.; Koehler, W. C. *Phys. Rev. Lett.* **1985**, *22*, 2425.
(34) de Gennes, P.-G. *Scaling Concepts in Polymer* Physics; Cornell University Press: Ithaca, NY, 1979.

Mixed-Crystal Infrared Spectroscopy of Annealed Solution-Grown Crystals of Polyethylene†

Stephen J. Spells*

Department of Applied Physics, Sheffield City Polytechnic, Pond Street, Sheffield S1 1WB, England

David M. Sadler

H. H. Wills Physics Laboratory, University of Bristol, Tyndall Avenue, Bristol BS8 1TL, England. *Received November 15, 1988; Revised Manuscript Received March 21, 1989*

ABSTRACT: The CD_2 bending vibration is analyzed in annealed solution-grown polyethylene crystals in terms of conformational changes. The results are compared with calculations from a range of models which involve "annealing zones" of various dimensions. The same model as was favored by neutron scattering measurements was found to give an adequate fit to IR data for moderate molecular weights (≤100 000). However, for higher molecular weights the IR band shapes show a better agreement with a model where the stems are preferentially removed from the ends of groups of adjacent stems. This discrepancy is discussed in light of possible refinements to the models. Analogous IR measurements on deuterated matrix samples show smaller reductions in CH_2 bending splittings on annealing, consistent with the suggested heterogeneity.[1]

Introduction

Wide-angle neutron scattering (WANS) measurements and Fourier transform infrared spectroscopy (FTIR) have recently been used in conjunction to obtain a detailed model of the chain conformation in solution-grown polyethylene (PE) crystals.[2-4] In combination with independent evidence, the possible ambiguity in describing the conformation was minimized. The same experimental techniques can now be applied to annealed single crystals, using our previous model for unannealed crystals as the starting point. Recent improvements in the method of calculating FTIR spectra on the basis of molecular models[5] can also be applied in this study of annealing.

Studies of the annealing behavior of PE single crystals are reviewed in more detail in the preceding paper.[1] The annealing falls into at least three distinct regimes. At the lowest temperatures (T_a), the number of crystal dislocations increases without any simultaneous increase in la-

† The work described in this paper represents a combined study undertaken over several years. David Sadler pursued the analysis of the neutron scattering results in 1987 and early 1988 and prepared an initial manuscript on which the present neutron scattering paper is largely based. I subsequently continued to analyze the infrared data and to make comparisons with molecular model calculations. Sadly, David's tragic death in 1988 prevented him from seeing how these fit his own conclusions. Consequently, the comparison of results from the two techniques and the conclusions drawn are the work of Stephen Spells.

0024-9297/89/2222-3948$01.50/0